

Role of cyclooxygenase-2 in vertebrate eye development

INTRODUCTION

Understanding the molecular and cellular mechanisms that govern eye development has important implications for treating a wide range of congenital disorders that can occur due to problems with the development of the eye, such as a condition in which one or both eyes fail to develop (anophthalmia) (Fig 5.1A). A condition in which one or both eyes are abnormally small is known as microphthalmia (Fig 5.1B). A variety of genetic or environmental factors are responsible for such types of abnormalities in the eye (Riordan-Eva & Cunningham, 2011). Another congenital eye defect is coloboma, which creates a hole in the eye tissue because of an improper closure of the optic fissure (Fig 5.1C). The abnormal growth of blood vessels in the retina can lead to vision loss or blindness. These are just a few examples of the many congenital disorders that can affect eye development. Early detection and treatment can be critical in preventing vision loss or other complications associated with these conditions.



Figure 5.1: Congenital eye defects in newborns (A) Anophthalmia, (B) Microphthalmia and (C) Coloboma in Humans (Mai et al., 2019)

The eye is a complex organ that allows us to see and interpret the world around us. Vertebrate eye development is a complex and highly orchestrated process that begins early in embryonic development. Eye development involves a coordinated growth and

differentiation of multiple tissues, including the retina, lens, cornea, iris, and optic nerve (Saha et al., 1992).

The vertebrate eye comprises various tissues from different embryonic origins, such as the iris and ciliary body, which developed from the wall of the diencephalon via the optic vessel and optic cup (Stenkamp, 2015). In contrast, the lens and cornea originated from the surface ectoderm. The coordinated action of transcription factors and inductive signals ensures the normal development of various eye tissues (Cvekl & Mitton, 2010).

During gastrulation, the growing eye is centrally located as a single-eye field. Shh splits the single eye field into two eye fields (England et al., 2006). After the initial induction of the neural ectoderm by the underlying archenteron, the first morphological indication of eye formation is an out pocketing of the diencephalon. The out pocketing of the diencephalon initiates optic vesicle morphogenesis, followed by optic cup formation. In chick embryos, the evagination of the optic vesicle begins very early, and the depressions appear in the open neural plate, where it widens out in the future forebrain region. These early depressions are called optic sulci. The initial shallow concavity deepens to form the primary optic vesicles (Martinez-Morales & Wittbrodt, 2009). After the neural plate in the brain region has been closed, the optic vesicles appear in external views of the reconstruction of the central nervous system as rounded protuberances from the lateral walls of the forebrain (Fig 5.2).

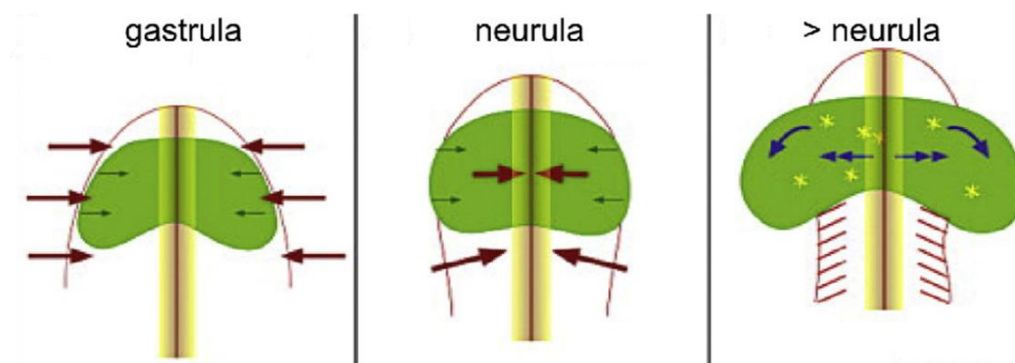


Figure 5.2: Differentiation of optic field (green patch) and movement of the cells (arrowhead) during early embryonic development of vertebrates (Sinn & Wittbrodt, 2013).

Optic cup

The lumen of the primary optic vesicle remains broadly continuous with the lumen of the forebrain, and the vesicle walls show little differentiation from the parent forebrain walls.

After that, the distal portion of the optic vesicle begins to flatten and becomes invaginated, leading to a single-walled primary vesicle transforming into a double-walled optic cup (Hyer et al., 2003). As the invagination was completed, the original lumen of the optic vesicle reduces to a vestigial slit between the inner and outer layers of the optic cup (Fig 5.3). At the same time, there is rapid differentiation of two layers of the optic cup (Picker et al., 2009). The outer layer becomes much thinner and begins to show melanin granules, indicating the formation of the retina-pigmented layer. The inner layer of the optic cup becomes much thickened, an indication of serial changes by which it will become the retina sensory layer. A sensory layer of the retina receives visual images and converts them into molecular signals (Nordquist & McLoon, 1991).

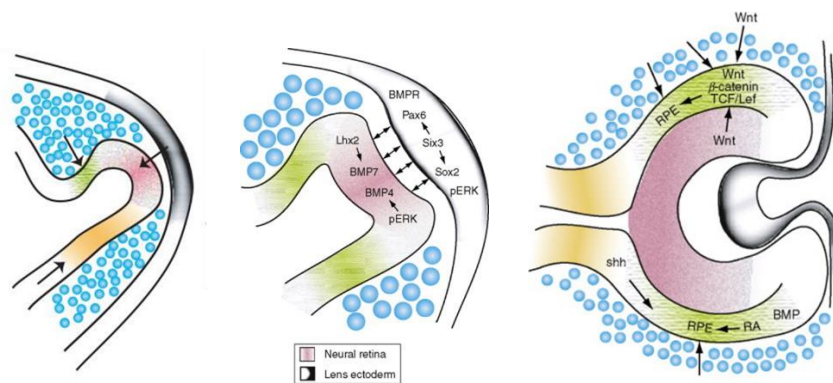


Figure 5.3: Signalling molecules aiding optic cup development (Fuhrmann, 2010)

In chick embryos, the optic cup does not form in the center of the optic vesicle but eccentrically towards its ventral margin, which makes a gap in the wall of the optic cup known as a choroid fissure (Nagata et al., 1988). The hyoid artery is partially enveloped by a choroid fissure which supplies blood to many structures of the developing eye. The optic stalk, along with part of the choroid fissure, is extended and invaded by nerve cells located in the sensory layer of the retina.

Formation of lens

Lens formation is a tightly regulated event of eye development where two cell layers interact and differentiate. The lens formation begins before the invagination of the primary optic vesicle (Grainger, 1992). As the optic vesicle forms, it comes into close contact with the overlying head ectoderm. The inductive event occurs in the head ectoderm and optic vesicle, leads to lens formation (Fig 5.3). Under the induction signals, the superficial

ectoderm overlying the optic cup begins to develop a local thickening known as lens placode (Donner et al., 2006). As the cavity in the optic cup deepens, the lens placode protrudes towards the optic cup and forms an open lens vesicle called a lens pit. Once the lens vesicle closes, it breaks away from the parent ectoderm and forms a lens. The rounded lens body in the optic cup opening starts elongating the cells and transforming into the long transparent elements known as lens fibers (Grainger, 1992).

As the lens increases in size, it settles back into the optic cup, and the margins of the cup begin to overlap its edges. The overlapping of optic cup proceeds along with the formation of epithelial portion of the iris and simultaneously a reduced opening in front of the lens as a pupil emerges (Piatigorsky, 1981). Outside the epithelial layer, loosely arranged mesenchyme will be organized into the muscular portion of the ciliary body. These ciliary muscles, by altering the tension on the suspensory ligament of the lens, control the lens curvature and thereby help the eye to change focus on creating a sharp image on the retina (Kröger et al., 1999). The outermost layer of the developing eye is the cornea, which is the epithelium derived from the superficial ectoderm that closes over the lens vesicle (Lwigale, 2015). An inductive influence emanating from the lens vesicle and the optic cup stimulates the transformation of ordinary surface ectoderm to corneal epithelium (Fig 5.4).

Molecular players of eye development

Eye development is an example of a reciprocal induction mechanism. It involves the precise coordination of various molecular and cellular events (Cvekl and Piatigorsky, 1996; Muta et al., 2002). Multiple genes and signaling pathways regulate eye development, including WNTs, BMPs and FGFs. WNT signaling pathway is involved in regulating the formation of the optic vesicle and the differentiation of the lens. Moreover, Fzd5 and WNT11 function to inhibit WNT signaling and promote eye field development in zebrafish (Cavodeassi et al., 2005). The formation of the eye field occurs at the anterior of the neural tube, where Otx2 inhibits WNT and BMP signaling, which define the eye field (Ramón Martínez-Morales et al., 2004). The neural tube is positive for WNT and BMP, but Noggin is present at the anterior region of the neural tube, which inhibits BMP and allows the expression of Otx2 (Bayramov et al., 2011). After defining the eye field optic vesicle was formed, and the dorsoventral axis of the optic vesicle was established by WNT7b (Parr et al., 1993).

The overlying surface ectoderm of the optic vesicle under the expression of *BMP4* leads to lens placode induction.

The optic vesicle also expresses *BMP7*, which interacts with the lens placode and forms the optic cup. A study in chick embryo showed that loss of function mutation in *BMP4* displayed the absence of a lens known as aphakia (Huang et al., 2015). Furthermore, *Pax6*, a transcriptional factor, plays a crucial role in eye development. It is expressed in the developing eye during early stages and regulates the optic vesicle, lens, and retina formation. *FGF8* is expressed in the optic vesicle and regulates the formation of the optic cup and the differentiation of retinal cells. During eye development, *Msx2* transcripts first appear in the optic vesicle (OV) and adjacent ectoderm in E9.5 mice (Wu et al., 2003). In zebrafish *ptch2* mutants, optic fissure and optic stalk cell movements are disrupted, resulting in a retina that lacks closely opposed fissure margins in the ventral eye. In other cases, coloboma-associated genes may also act early during eye development but play more general roles in the growth or patterning of the optic cup (Bibliowicz et al., 2011; Morris, 2011; Gestri et al., 2012).

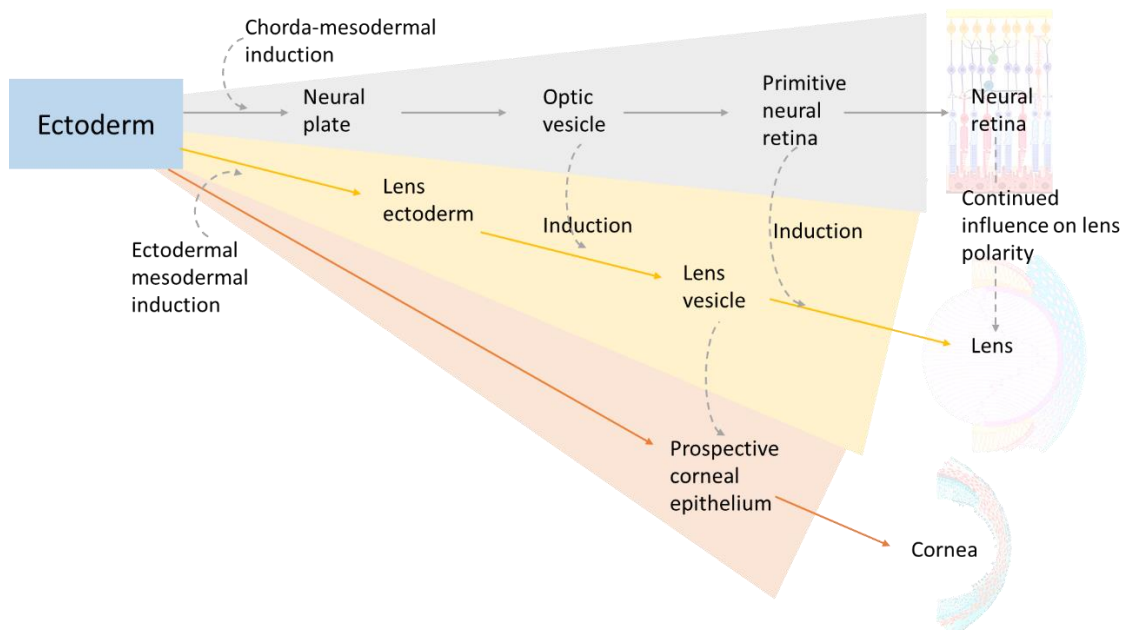


Figure 5.4: Molecular regulators of eye development (derived from Graw, 2010)

The optic cup differentiates into the retina, which is of two types: neural retina, the thick inner layer of the optic cup and pigmented retina, the thin outer layer of the optic cup (Fig 5.4). Induction and development of both the layers of the retina appear to be mediated by fibroblast growth factors (FGFs) expressed in the surface ectoderm and distal optic vesicle

(Pittack et al., 1997; Hyer et al., 2003; Nguyen and Arnheiter, 2000; Vogel-Höpker et al., 2000; Martinez-Morales et al., 2003). The canonical WNT signalling pathway (WNT11) plays a role in regulating the proliferation of retinal progenitor cells and their differentiation into different types of retinal cells. *Xenopus* neural retina development occurs through canonical WNT signaling via the Fz5 receptor (Van Raay & Vetter, 2005). Furthermore, in zebrafish, WNT2b and WNT8 are expressed in the dorsal retinal pigment epithelium (RPE), and numerous members of the Tcf family of transcription factors that mediate WNT signalling are dynamically expressed in the developing eye (Veien et al., 2008).

Along with the WNT pathway, different isoforms of BMPs and FGFs are involved in regulating the formation of the optic cup and the differentiation of retinal cells (Wu et al., 2003; Atkinson-Leadbetter et al., 2014). Lens placode ectoderm secretes FGF10 that instructs the optic cup to activate neural retina differentiating gene *Vsx2* (Zagozewski et al., 2014). FGF9 is expressed in the developing retina and is involved in regulating retinal cell differentiation, including the formation of photoreceptors (Zhao & Overbeek, 2001).

The microphthalmia-associated transcription factor (MITF), a basic helix-loop-helix leucine zipper transcription factor essential to acquiring and maintaining RPE cell identity, has been studied extensively (Martinez-Morales et al., 2009). Mesenchymal cells adjacent to optic vesicles activate MITF, leading to pigmented retina differentiation (Fuhrmann, 2010). Along with that, members of the orthodenticle-related family of transcription factors, *Otx1* and *Otx2*, are essential for RPE differentiation during the development of the vertebrate eye (Martinez-Morales et al., 2001; Martinez-Morales et al., 2003). *Otx1* and *Otx2* are expressed throughout the optic vesicle during initial eye development. Which later concentrates only on presumptive RPE and persists in adult RPE (Martinez-Morales et al., 2009). In *Otx1/Otx2* mutants, RPE formation is disrupted, and the outer layer of the optic cup acquires neural retina-like characteristics (Acampora et al., 1999).

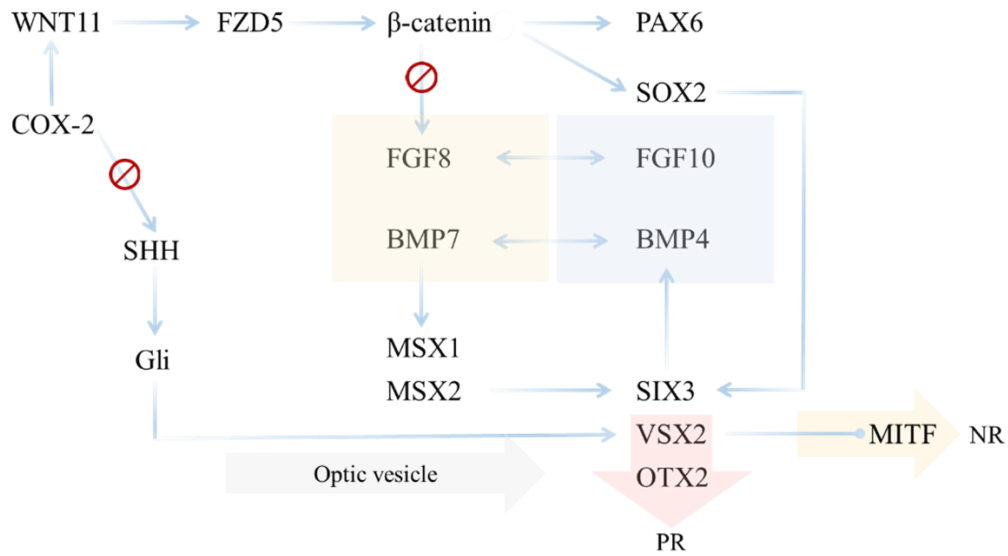


Figure 5.5: Major molecular interactions of eye development in the chick embryo

Differentiation of retina and lens are two simultaneous processes that coincide when the signals from the optic cup which induce the lens formation in the overlying lens placode. Optic vesicle cells flattened against the surface ectoderm and produce BMP4, FGF8 and Delta that convert surface ectoderm to lens placode (Furuta & Hogan, 1998; Esteve & Bovolenta, 2006; Perron & Harris, 2000). Along with that WNT/ β -catenin pathway is involved in the differentiation of the lens epithelial cells. The mouse with LRP6 insertional mutation displayed microphthalmia and coloboma, implicating the involvement of canonical WNT signalling (Zhou et al., 2008). BMP7 regulates the differentiation of lens epithelial cells into lens fiber cells, which is essential for forming a transparent lens (Hung et al., 2002). BMP7 expresses prior to lens placode induction in an optic cup and later in development. Another isoform, BMP4, has been linked to the development and differentiation of the lens because it is genetically upstream of Sox2, which controls the expression of crystalline genes (Wawersik et al., 1999, Kamachi et al., 2001). BMP4 does not regulate the expression of Pax6, but it is necessary for the upregulation of Sox2 (Furuta and Hogan, 1998), a transcription factor that regulates the expression of crystalline genes in combination with Pax6 (Kamachi et al., 2001). During early lens induction, FGF signalling is essential for regulating Pax6 expression in lens placodes (Faber et al., 2001). Mouse Pax6 homozygous mutants have only remnants of ocular tissues and die shortly after birth due to nasal dysfunction, whereas heterozygous mutants have small eyes. FGF8 secreted by the optic cup maintains the crystalline gene expression, which is the major

protein of lens cells (Reza et al., 2007). During lens formation, lens epithelial cells express MSX2 and help in the differentiation of the lens fiber cells in mice (Yu et al., 2018).

Despite extensive research on embryonic eye patterning, congenital eye abnormalities, underlying cell dynamics, and their causes remain unexplained (Adler and Canto-Soler, 2007; Fuhrmann, 2010; Martinez-Morales et al., 2004). Among all the factors regulating eye development, a relatively new molecule is cyclooxygenase 2 (COX-2), a member of the cyclooxygenase enzyme family. COX family has two isoforms, COX-1, COX-2 and one splice variant, which is widely known as COX-3. These enzymes are responsible for converting free arachidonic acid into prostaglandins. COX-1 is usually expressed in all cell types and maintains the basal level of prostanoids (Morita, 2002). In contrast, the expression of COX-2 occurs under the influence of inflammatory mediators and hormones which promotes prostaglandin synthesis. In addition, COX-2 is extensively studied in cancer progression and tumor cell metastasis. The role of COX-2 in cellular events is known to regulate cell proliferation by interacting with WNT signaling in lizard tail regeneration (Buch et al., 2018). Additionally, COX-2 promotes the differentiation of keratinocytes and the mobility of the cytoskeleton in bladder cancer cells (Leong et al., 1996). Despite knowing many roles of COX-2 in cellular events, the role of COX-2 in embryonic development has not been explored. Hence, we have investigated the role of COX-2 in embryonic development. Previous laboratory studies demonstrated the presence of COX-2 in somites, eyes, the heart tube, the midbrain, the limbs, and the kidneys (Verma et al., 2021). As eye development is a complex process, the role of COX-2 in eye development is unexplored. This study was conducted to determine the role of COX-2 in eye patterning. The significance of COX-2 in early eye patterning in chick embryos was investigated by inhibition and deletion studies.

MATERIALS AND METHODS

Initially, COX-2 inhibition was carried out by using the pharmacological inhibitor Etoricoxib. Freshly laid fertilized RIR eggs were separated into two groups, namely control and treatment. The treatment group of eggs were treated with etoricoxib and allowed to develop till HH12, HH14 and HH16 stages. The isolated embryos of both groups were checked for morphology, followed by COX-2 activity test. Morphological features of the control and treatment group of embryos were recorded as images.

In situ hybridization

Embryos from a control group of eggs were isolated in ice-cold PBS at HH12, HH14 and HH16. Isolated embryos were fixed with 4% PFA for 2-3 hours at room temperature and washed in PBS 2-3 times. Then embryos were passed through a methanol gradient and final storage in 100% methanol at -20°C.

Probe designing

To generate templates for COX-2 riboprobes, RNA was extracted from HH14 chicken eyes using the TRIzol method and cDNA was synthesized using Superscript III (ThermoFisher Scientific, USA) according to the manufacturer's instructions. DNA fragments were isolated by PCR (94°C for 5 min, 35 cycles of 94°C for 40 s, 55°C for 1 min, 72°C for 90 s, followed by a final extension at 72°C for 5 min) and cloned into pGEM-T Easy (Promega, USA). The following primers were used for COX-2

Forward: GGGGCGTAGGTGTTCTGTTT

Reverse: GCCAGGCCCTTTCTTATGGT

RNA probes for COX-2 were designed using a DIG RNA labelling mix (Roche, USA). The plasmid was isolated, and the alignment of the sequence was checked. The concentration of the plasmid was checked before using it for probe synthesis. The following reaction mixture was used for probe synthesis:

Reagents	Volume (µl)
DIG RNA labelling mix (10X)	2
Transcription buffer (10X)	2
T3 RNA polymerase	2
linearized plasmid with 0.5µg concentration	6
sterile RNase-free double distilled water	8
Total	20

The tubes were incubated for 2 hours at 37°C. After adding 2µl of DNase I RNase free to remove template DNA from the tube, the mixture was incubated for 15 minutes at 37°C. The reaction was stopped by adding 2µl of 0.2M EDTA (pH 8.0).

Probes that were synthesized, were subsequently treated for ethanol precipitation. In synthesized probes, 2µl of 4M LiCl and 100µl of 100% pre-chilled ethanol were added. The tubes were incubated for 5-6 hours at -20°C. Tubes were centrifuged at 13000g for 5 min at 28°C and collected the pellet after decanting the supernatant. The pellet was washed once again with 70% ethanol. The pellet was collected, briefly dried in a vacuum, dissolved in 75µl RNase-free double-distilled water, and kept at -20°C.

Labelled RNA probes were purified using small quick spin columns (Roche, USA). The columns were prepared by re-suspending the matrix and spinning at 1000rpm for 1 minute to remove the residual buffer and pack the column. The labelled RNA probes were pored to the centre of the column bed and spun at 1,000 rpm for 1 minute. The elute contained purified probes, which were immediately stored at -80°C. The quality and quantity of purified probes were assessed using agarose gel electrophoresis and Nanodrop.

Hybridization

The hybridization of the probe was a three-day procedure given below in day wise manner:

Day 1:

The embryos in methanol were rehydrated with PBS-Hit solution (PBS + 0.25% tween20 solution) after rehydration, and embryos were washed in PBS-Hit for 5 minutes 3 times.

Rehydrated embryos were treated with Proteinase K (10µg/ml) on ice for 10 min. The Embryos were rinsed carefully in PBS-Hit solution for 5 min 2 times at room temperature. The embryos were re-fixed in 4%PFA + 0.2% glutaraldehyde in PBS for 1 hour. After fixation, embryos were rinsed with PBS-Hit for 5 minutes 3-4 times.

Embryos were transferred to a pre-hybe solution and kept till the embryos sank. Once the embryos sank, freshly prepared pre-hybe was added and kept at 65°C for 1 hour. After one hour, the pre-hybe of the embryo was replaced with RNA probes diluted in pre-hybe and kept at 65°C overnight.

Day 2:

On the following day pre-hybe probe solution was removed, and a wash solution was added to remove unbound probes. The embryos were kept in a wash solution for 30 minutes, four times at 65°C.

Embryos were washed in 50/50 wash solution/MABT solution mixture at 65°C for 15 minutes. Further embryos were washed in MABT solution for 30 minutes 3 times at room temperature.

The non-binding sites in embryos were blocked using MAB-Hit with 2% BBR for 1 hour at room temperature. Further blocking was done using MAB-Hit with 2% BBR and 20% goat serum for 1 hour at room temperature. The blocking solution was replaced with an antibody (anti-DIG fab) diluted (1:2000) in MAB-Hit and incubated overnight at 4°C.

Day 3:

The embryos were removed from the antibody solution, and excess antibodies were washed away using MAB-Hit solution for 30 minutes five times. The last wash with MAB-Hit was extended overnight at 4°C.

Further, the embryos were washed with NTMT solution for 10 minutes twice. After washing with NTMT, the embryos were transferred into a colorimetric solution and kept in the dark.

Embryos were observed every hour, and once the color developed reaction was stopped by changing the solution to PBS-T. Multiple PBS-T washes were given to the embryos to remove further background staining.

Once the optimum color developed, the embryos were photographed and stored in 60% glycerol in PBS for an extended period.

The stained embryos were processed for sectioning as well. The sections were washed twice with PBS-T, mounted on a slide, and imaged under the light microscope.

Reagents:

- Pre-Hybe solution (50 ml)

Formamide	25ml
SSC pH 5 (20X)	3.25ml
EDTA (0.5M)	0.5ml
Tween 20 (25%)	0.5ml
CHAPS (10%)	2.5ml
yeast RNA (20 mg/ml)	250 μ l
Heparin (50 mg/ml)	100 μ l
Volume make-up with de-ionized water up to 50ml	

Wash Solution (50 ml)

Formamide	25ml
SSC pH 5 (20X)	2.5ml
Tween (25%)	0.5ml
Volume make-up with de-ionized water up to 50ml	

MABT remember to pH to 7

Maleic Acid	100mM
Sodium Chloride	150mM
Tween-20	0.25%

NTMT (50 ml)

Tris pH 9.5 (1M)	5ml
MgCl ₂ (1M)	2.5ml
NaCl (5M)	1ml
Tween (25%)	2ml
Volume make-up with de-ionized water up to 50ml	

Embryo manipulation

Another part of the study was carried out by deleting COX-2 in optic vesicle and optic cup using CRISPR/Cas9 system. Guide RNA for COX-2 was generated using Breaking-Cas (Juan et al., 2016) for Exon4, which encodes the active site of the COX-2 enzyme. Deletion

of exon 4 generates the truncated protein, which is non-functional. The synthesized gRNA of COX-2 and control were inserted into the CAG-eCas9-GFP-U6-gRNA vector using BbsI single enzyme digestion (Fig 5.6), followed by transformation and cloning of plasmid. The transformed colonies were picked up, and the plasmid was isolated. The isolated plasmid was checked for gRNA insert and alignment through PCR and sequencing. The one with a correct insert of gRNA was carried forward for an experiment.

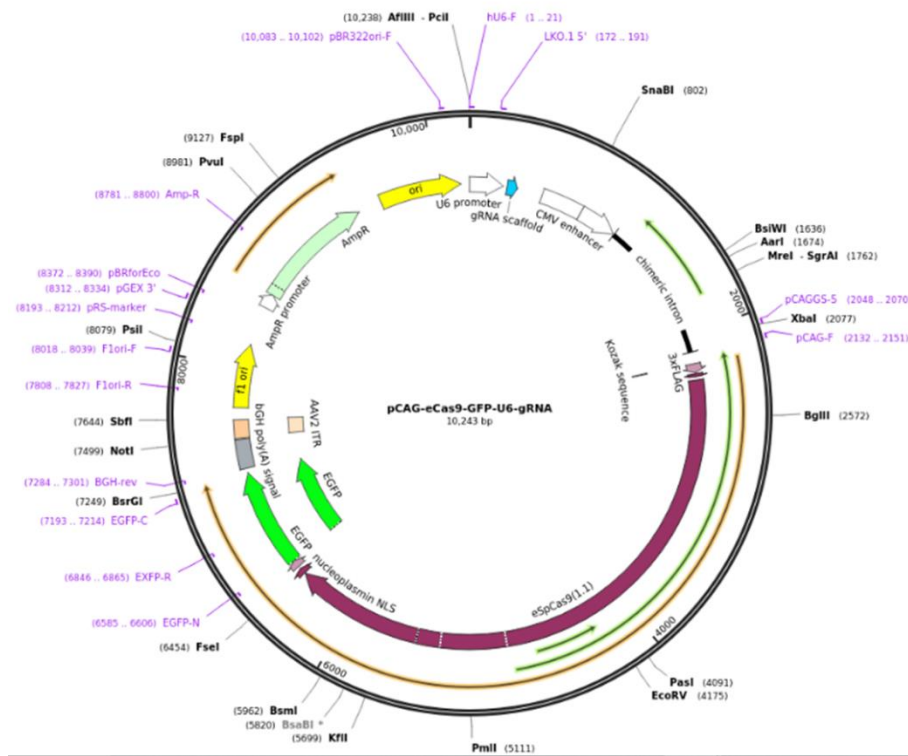


Figure 5.6: pCAG-eCas9-U6-gRNA vector (<http://n2t.net/addgene:79145> ; RRID:Addgene_79145)

The eggs were first incubated at 37°C with 50% humidity for 4-6 hours. The embryos were then isolated using a filter ring and placed on a plate electrode that was submerged in Ringer's solution (Fig 5.7). The extraembryonic membrane was removed from the anterior region of the embryo using a pair of forceps. A mixture of gRNA-Cas9 plasmid, 30% sucrose and 1% fast green was injected using a micropipette onto the top of the optic placodes. Another electrode was placed parallel to the dorsoventral axis of the embryo and electroporated at 7V for 5 pulses for 100ms each. The electroporated embryos were placed on an albumin agar plate and incubated at 37°C. Embryos at stages HH12 and HH14 were isolated and checked for COX-2 deletion through PCR and sequencing. The deletion-confirmed embryos were then analyzed for morphological observation.

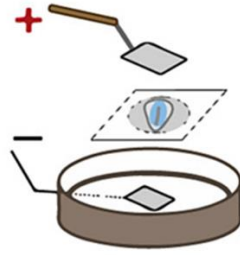


Figure 5.7: Electroporation of plasmid in HH4 stage embryo

The primary regulatory proteins responsible for eye development, such as β -catenin, Shh, Paax6, Fgf8, Fgf9 and R-cadherin, were checked through western blot at HH12, HH14 and HH16 stages.

RESULTS

Optic cup express COX-2

To test the idea that COX-2 has a role in patterning early eye development, we used *in situ* hybridization to analyze the expression of COX-2 in developing optic cups and lenses of control embryos. COX-2 is expressed strongly in developing optic vesicles at the HH12 stage (Fig 5.8). At HH14 and HH16 stages, the COX-2 is expressed in an optic cup and lens region (Fig 5.8).

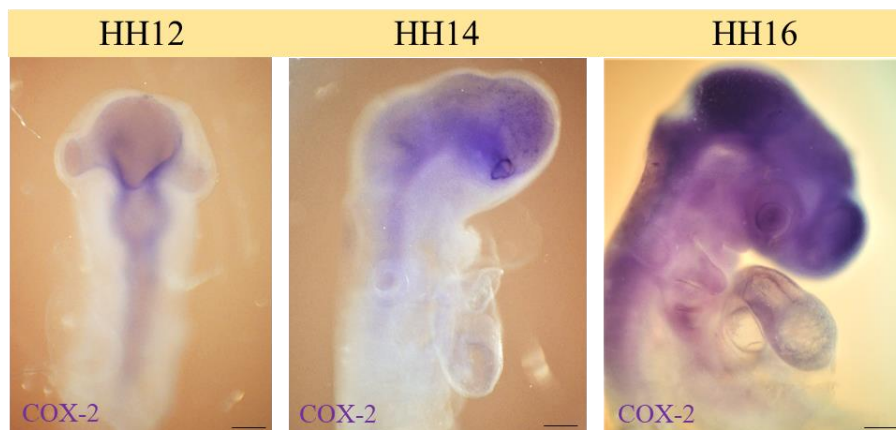


Figure 5.8: *In situ* hybridization of COX-2 in HH12, HH14 and HH16 stages of control group of embryo (4X). The purple coloration depicts presence of COX-2 mRNA

Further, COX-2 was localized into the sections of developing optic vesicles and an optic cup of control embryos. At the HH12 stage, COX-2 was localized at the neural ectoderm region of the developing optic vesicle, followed by HH16 stage COX-2 localized at the

surface ectoderm and lens placode. Later, the COX-2 was found to express in lens ectoderm at the HH16 stage (Fig 5.9).

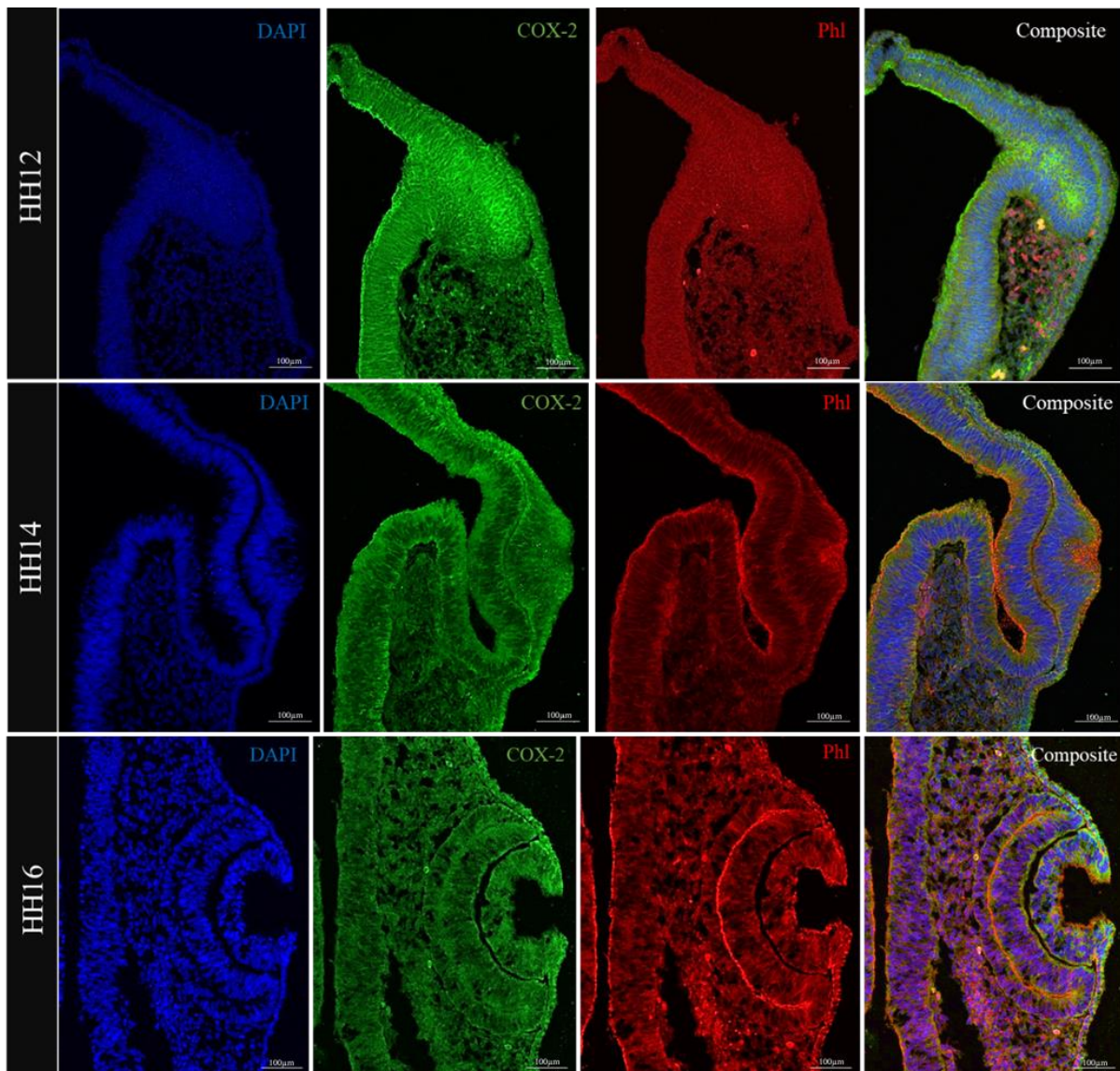


Figure 5.9: COX-2 localization in developing optic cup of HH12, HH14 and HH16 stages in control group of embryos. COX-2 counter stained with DAPI and Phalloidin on all the stages (Blue-DAPI, Green-COX-2, Red-Phalloidin)

Moreover, in developing eye regions, COX-2 activity was checked through COX-2 activity assay at three early eye development stages (HH12, HH14 and HH16). At HH12 and HH14, the COX-2 showed high activity and reduced a little at HH16 (Fig 5.10). The etoricoxib-treated group of embryos also checked for COX-2 activity, which showed a significant reduction in the activity compared to control embryos (Fig 5.10, Table 5.1).

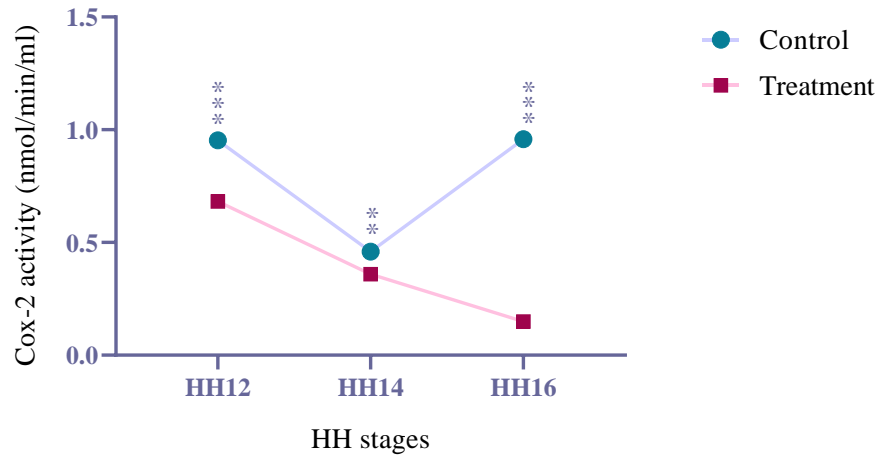


Figure 5.10: The COX-2 activity in developing optic vesicle and optic cup at HH6, HH12 and HH16 staged control and etoricoxib treated embryos; ** $p \leq 0.01$; *** $p \leq 0.001$

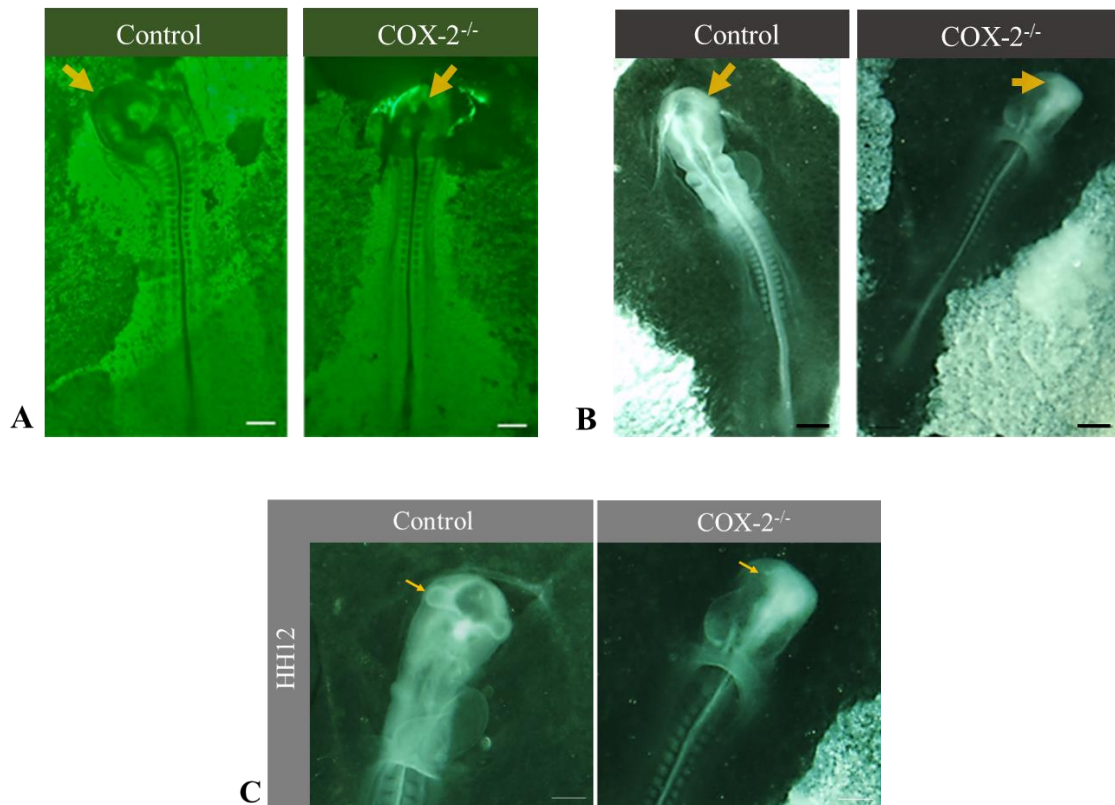


Figure 5.11: Cas9 mediated deletion of COX-2 of HH12 staged embryo. (A) Control embryo have normal developing head and no fluorescence (yellow arrow head); COX-2^{-/-} embryo showed fluorescence in the head region indicates the deletion of COX-2 (yellow arrow head). (B) The bright field image of HH12 stage control embryo with well developed optic cup (yellow arrow head) and COX-2^{-/-} deleted embryo showed poorly developed and unilateral absence of optic cup (yellow arrow head). (C) Bright field image of anterior region of the developing embryo of control and treated group at 10X magnification (Yellow arrow head).

It has been observed that the deletion of COX-2 during the development of embryos using Cas9 causes defective morphogenesis of the craniofacial region. As a result, the optic cups fail to develop and many embryos die before reaching the HH12 stage due to severe deformities in the craniofacial morphology. In addition to this, many embryos also exhibit distorted head structures after the deletion of COX-2 as compared to the control gRNA electroporated embryos (Fig 5.11).

Inhibition of COX-2 alters the eye morphogenesis

To understand the role of COX-2 during the development of optic cup and lens, morphological analysis was done where the characteristics were compared between the control and etoricoxib treated group of embryos at HH12, HH14 and HH16 stages of development.

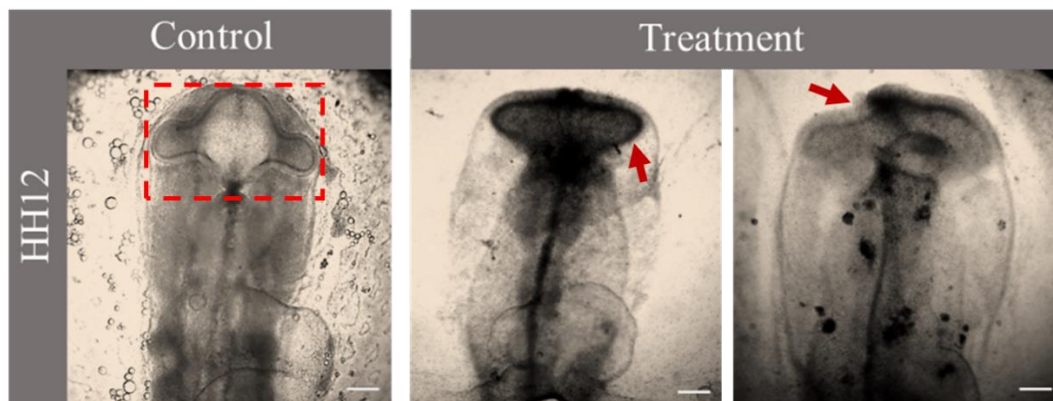


Figure 5.12: Morphology of optic vesicle at the HH12 stage of the developing embryo. Control embryo has well developed optic vesicles along with the brain regions (red dotted box) Etoricoxib treated embryos have defective optic vesicle development (red arrow head)

Control embryos of the HH12 stage have two distinct optic vesicles formed laterally to the forebrain region. However, optic vesicle formation prematurely ceased in the treatment group of embryos (Fig 5.12). In many embryos of the treatment group, the complete absence of optic vesicle formation was observed (Fig 5.12). At the HH14 stage, the control embryos had distinct optic vesicles, and the distal part was converted to an optic cup which started the lens induction. The treatment group at the HH14 stage showed bulged optic vesicles and the absence of optic cup formation. Few embryos showed short optic vesicles (Fig 5.13).

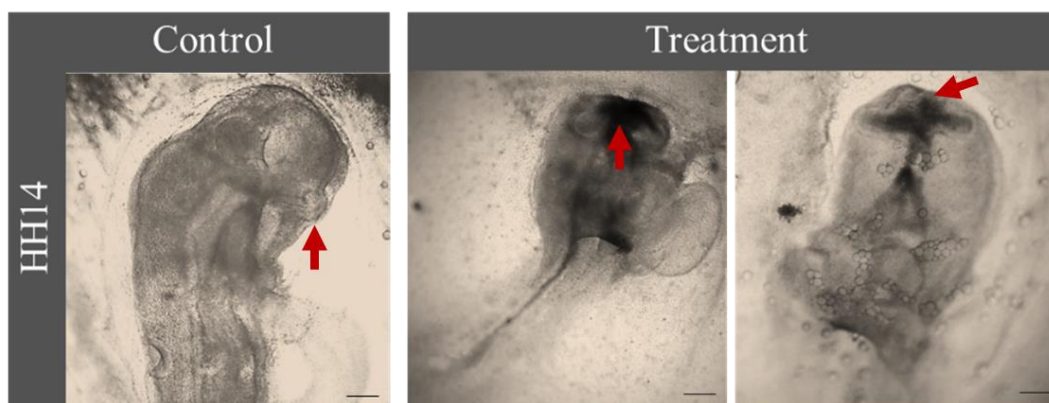


Figure 5.13: Morphology of optic cup at HH14 stage embryos. Control embryos with normally developed optic cup (red arrow head). Treatment embryos have complete absence of optic cup and unilateral optic vesicle formation (red arrow head)

With progression in development, the HH16 embryos are marked with differentiation of the optic cup into two distinct layers of the retina, which is visible in the control embryos' optic cup along with the lens. Conversely, optic vesicles when observed in the treatment group of embryos of the HH16 stage, did not progress to the optic cup formation and disrupted forebrain development was also observed (Fig 5.14). While in a few embryos, the entire optic vesicle was absent (Fig 5.14).

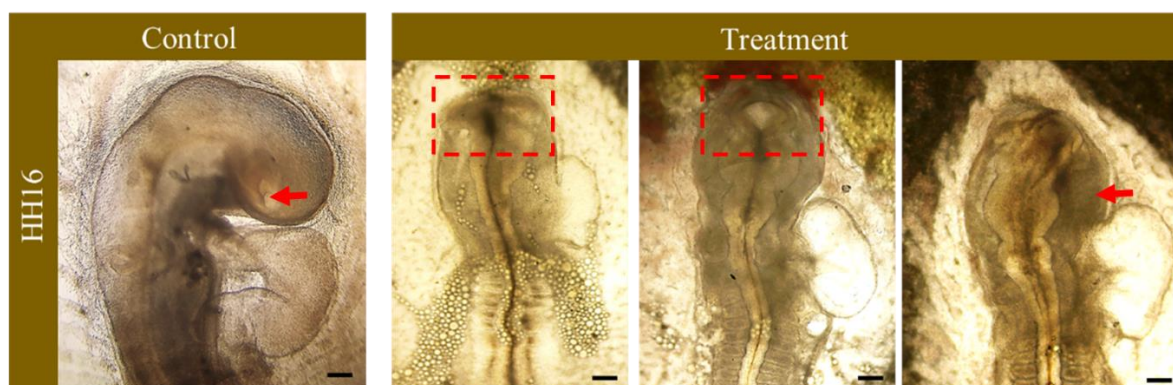


Figure 5.14: Morphology of eye at HH16 stage embryos. In control embryo optic cup differentiates into various tissues (red arrow head). In etoricoxib treatment group the growth of optic vesicle stopped and no further optic cup development (red dotted box)

Inhibition of the COX-2 alters the transcript levels of patterning eye

The levels of major transcription factors and ligands were quantified through real-time qPCR. We first determined the expression of *WNT11*, *Fzd5*, *BMP4* and *BMP7*. At the HH12 stage significant increase in the expression of *WNT11* and *Fzd5* was found in the treated group of embryos (Fig 5.15). In contrast, *BMP4* and *BMP7* showed a non-*COX-2* and the vertebrate eye

significant increase in expression. Additionally, expression patterns of *FGF8*, *FGF9*, *SHH*, *SOX2* and *PAX6* along with transcriptional factors like *MSX1*, *MSX2*, *SIX3*, *VSX2*, *OTX2*, *MITF*, *DELTA* were checked during all the three stages of eye development (Table 5.2).

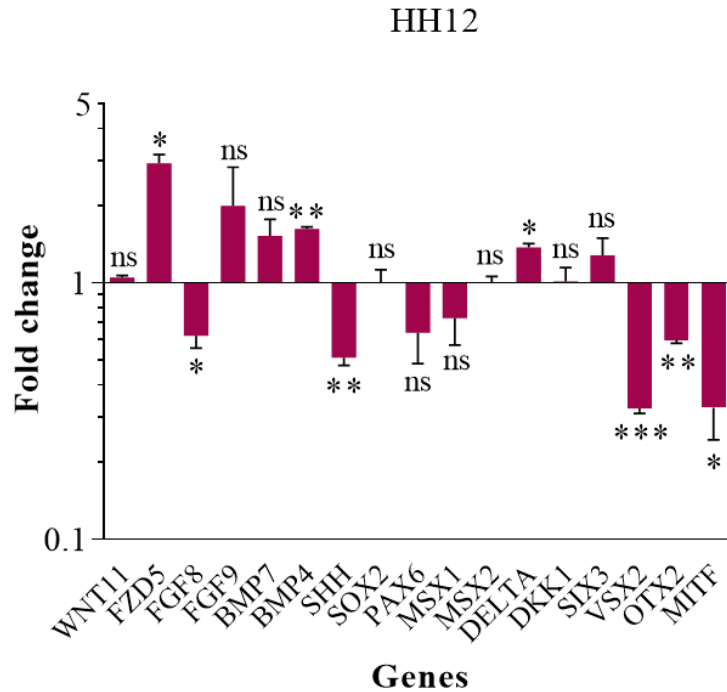


Figure 5.15: Regulatory gene expression of HH12 stage under inhibition of COX-2. The fold change value for the control embryo is 1.0 for all the genes, n=3, with 30 eggs per group per stage; ns-non significant; ns=non significant; * $p \leq 0.05$; ** $p \leq 0.01$; *** $p \leq 0.001$

At the HH12 stage, etoricoxib-treated embryos indicated a significant reduction in *SHH*, *FGF8* and *MSX1*, compared to control ones. Meanwhile, *WNT11*, *FZD5*, *FGF9* and *BMP7* showed a remarkable increase in the treated group. *MSX2*, *SOX2* and *DELTA* transcripts increased negligibly in the treated embryos, along with a non-significant rise in the *SIX3* gene expression at the HH12 stage compared to the control group (Fig 5.15). A noticeable reduction in *VSX2*, *OTX2* and *MITF* gene expression was observed in COX-2 inhibited group of embryos at the HH12 stage (Fig 5.15, Table 5.2).

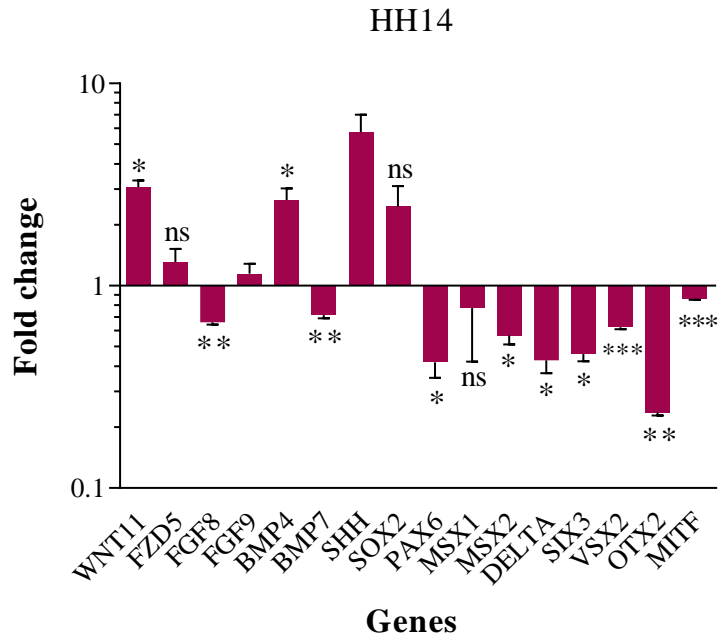


Figure 5.16: Gene expression of regulatory molecules on HH14 stage of developing control and treated embryos under inhibition of COX-2. The fold change value for the control embryos is 1.0 for all the genes, n=3, with 30 eggs per group per stage; ns=non significant * $p \leq 0.05$; ** $p \leq 0.01$; *** $p \leq 0.001$

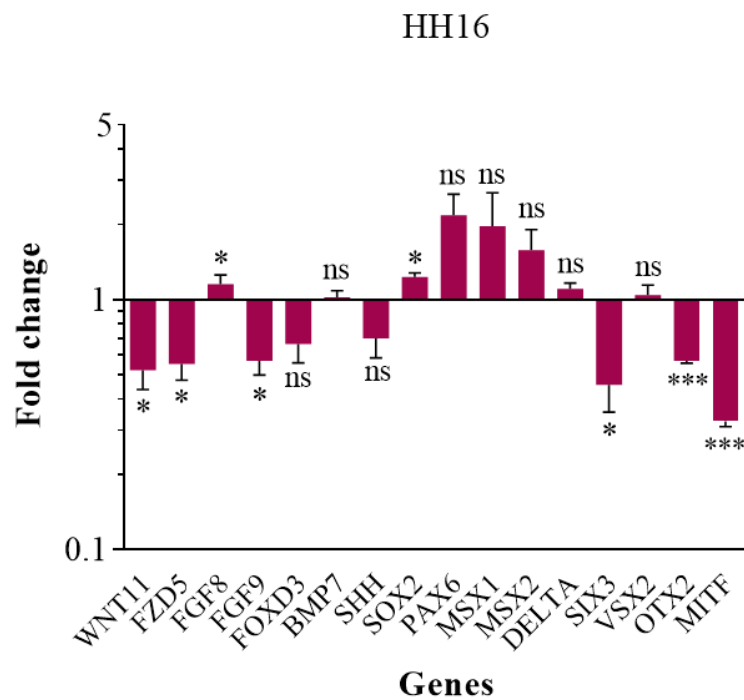
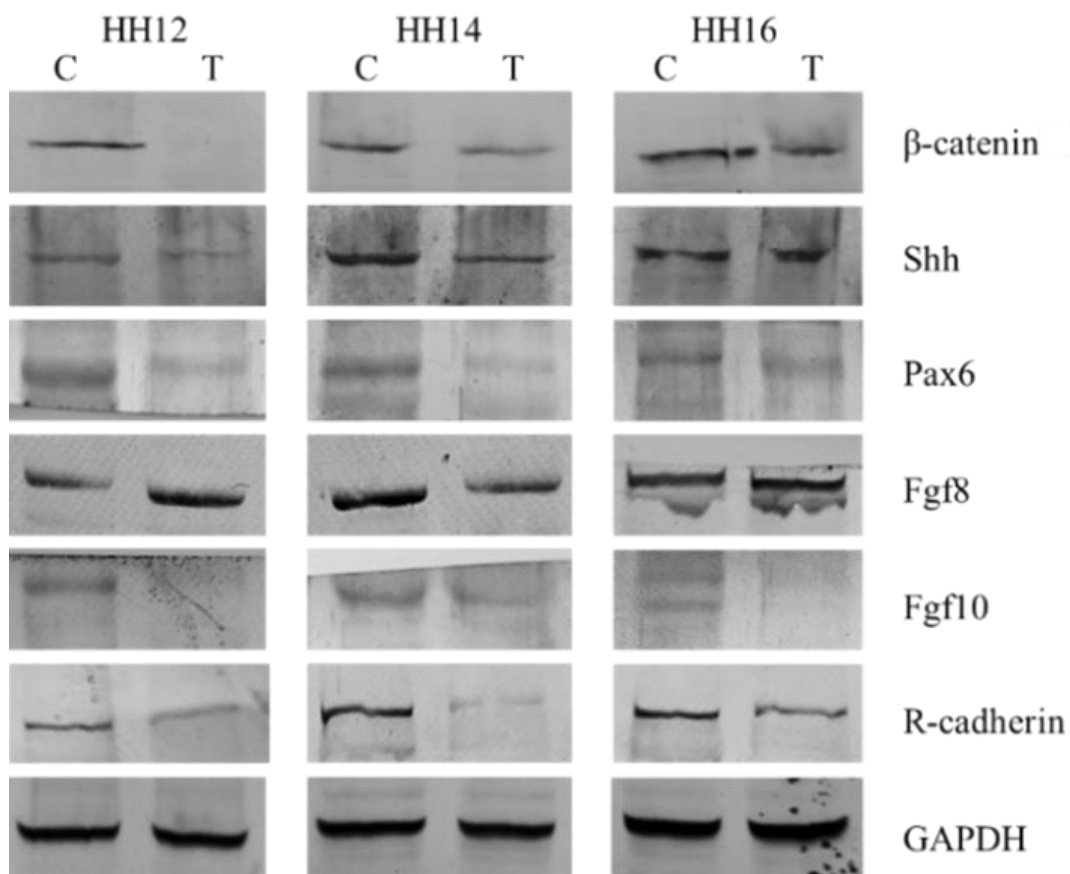


Figure 5.17: Gene expression of regulatory molecules on HH16 stage of developing control and treated embryos. The fold change value for the control embryos is 1.0 for all the genes, n=3, with 30 eggs per group per stage; ns=non significant; * $p \leq 0.05$; ** $p \leq 0.01$; *** $p \leq 0.001$

At the HH14 stage, treated embryos showed a non-significant increase in *SHH*, *SOX2*, *FGF9*, *MSX1* and *OTX2* compared to control ones. At the same time, *WNT11*, *FZD5* and *BMP4* increased significantly whereas, downstream of that, *FGF8*, *PAX6*, *MSX2*, *Delta*, *VSX2*, and *MITF* showed a remarkable decrease in expression as compared to the control group (Fig 5.16, Table 5.3). Further, as development proceeded at HH16, the expression pattern of the genes responsible for optic cup development changed under inhibition of COX-2. At HH16, expression of *WNT11* and *FZD5* decreased, whereas *PAX6*, *MSX1*, *MSX2*, *DELTA*, *SIX3* and *BMP7* non-significantly increased in the treatment group compared to the control group (Fig 5.17). The expression of *FGF8* and *SOX2* elevated significantly; however, another member of the fibroblast family, *FGF9*, decreased along with *BMP4*, *VSX2*, *OTX2* and *MITF* in treated embryos compared to control embryos (Table 5.4).

Protein expression in COX-2 inhibited group of embryos

The proteins regulating eye morphogenesis, such as β -catenin, Shh, Pax6, Fgf8, Fgf10 and R-cadherin, were checked through western blot in the control and treated group of embryos. The densitometric analysis of western blot revealed a significant decrease in the expression of β -catenin at the HH12 and HH14 stages of development in the etoricoxib-treated embryo. At HH16, the levels of β -catenin were restored to normal in the treatment group of embryos. The treatment group of embryos downstream of β -catenin, such as Pax6, also showed a significant decrease at HH12, HH14 and HH16 stages compared to the control group.



Volcano Plot

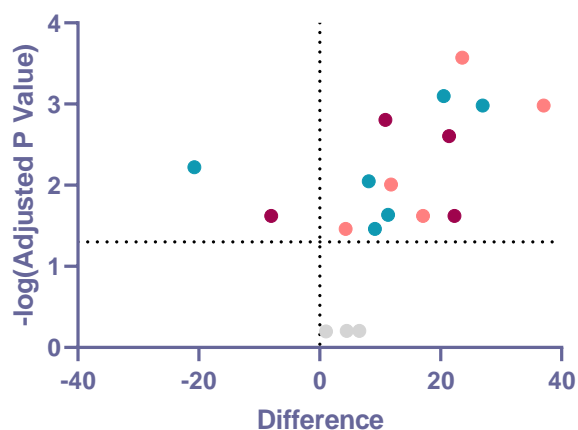


Figure 5.18: Western blot of protein regulating eye development & volcano plot (blue spot-HH12, pink spot-HH14, red spot-HH16) of the significant difference in protein levels in control and treatment group of embryos. The grey spots indicate nonsignificant values for HH12, HH14 and HH16).

Another regulatory molecule of eye patterning, Shh, showed deviant expression under COX-2 inhibition; at HH12 and HH14 stages, it decreased significantly compared to a control group. However, at the HH16 stage, Shh levels escalated non-significantly in the treatment group of embryos. Further, molecular cross-talk of Fgf8 and Fgf10 during optic

cup development was altered when COX-2 was inhibited in developing embryos. At the HH12 stage, Fgf8 increased and was followed by the HH14 stage; it declined drastically and again at the HH16 stage, it returned to normal levels in the treatment group of embryos. Fgf10, a companion molecule of Fgf8 at the HH12 and HH16 stages, declined significantly, but at the HH14 stage, it rose non-significantly in the etoricoxib-treated group of embryos (Fig 5.18, Table 5.5). Additionally, retina differentiation marker R-cadherin was checked, which showed a significant decrease at all three stages (HH12, HH14 and HH16) of developing eye in COX-2 inhibited group compared to the control group.

DISCUSSION

The formation of functional organs requires the integration of tissue with different embryonic origins, which is evident in vertebrate sense organ development, and one such organ is the eye. Although it has been known for over 50 years that eye development is a complex regulatory mechanism, the underlying process has proven to be elusive, and the current findings add to the knowledge of early eye morphogenesis of vertebrates.

The present study provides new evidence that COX-2 is present during early eye morphogenesis and regulates cellular events by interacting with different signalling molecules. During early eye development, WNT11 express in the presumptive lens placodes and later in the periocular mesenchyme of the optic vesicle (Carpenter et al., 2015). Additionally, WNT/ β -catenin signaling regulates the PAX6 expression in lens placode to form a lens from surface ectoderm in *Xenopus* (Rasmussen et al., 2001). Buch and colleagues illustrated that inhibition of COX-2 alters WNT/ β -catenin signaling, which hampers lizard tail regeneration (Buch et al., 2018). Here at the HH12 and HH14 stages, where optic vesicles and optic cups are formed, the expression of WNT11 and FZD5 increases under inhibition of COX-2. Laterally the levels of β -catenin were also checked at the same stage, and it was significantly decreased in developing optic vesicles when COX-2 was not active. The altered levels of WNT/ β -catenin in etoricoxib-treated embryos lead to abnormal optic vesicle development at the HH12 stage in chick embryos. Further, at the HH16 stage under COX-2 inhibition, levels of WNT11 along with FZD5 significantly decreased, and β -catenin expression declined marginally, indicating the major signaling alteration. PAX6 and SOX-2 define the neural retina and optic cup through gradient

expression. However, due to COX-2 inhibition, the gradient has been lost, and no retina and optic cup specification occurred at the HH16 stage.

BMPs and FGFs are known to play an essential role in patterning the optic cup and retina (Adler & Canto-Soler, 2007; Zhang et al., 2002). The BMP4 transcript is present in both the presumptive lens and the presumptive retina. Still, it is expressed predominantly in the dorsal optic cup as primary fiber cell differentiation begins at E11.5 in mice (Furuta & Hogan, 1998). The mRNA levels of BMP4 elevated during the initial stages (HH12 and HH14) of eye development in etoricoxib-treated embryos. With that, BMP7 also increased expression at all three stages of eye development under COX-2 inhibition, leading to early lens induction in surface ectoderm and defective lens formation. FGF8 and FGF9 are necessary for maintaining cell proliferation in the presumptive retina and later for corneal development (Vogel-Höpker et al., 2000). During early patterning of the eye transcript, levels of FGF8 expression declined, which gradually rose and came to normal levels, whereas FGF9 rose and slowly came down in the absence of COX-2. Due to the amended expression of both FGFs, cell number decreases, and a defective retina is formed.

Shh is known as the eye field splitting molecule, and inhibition of Shh leads to the formation of one eye (cyclopia) in embryos (Sasagawa et al., 2002). The embryos lacking COX-2 exhibited cyclopia and therefore the expression levels of Shh too were checked. Under ablation of COX-2, expression of Shh decreased at the HH12 stage, followed by a marginal increase at the HH14 stage and again declined at the HH16 stage. The expression pattern of the Shh indicated that the initial phase of eye field splitting did not have enough Shh levels, which might lead to single-eye formation. Msx1 has been linked to Pax-6 expression during eye formation and nasal placodes in vertebrates (Grindley et al., 1995).

Similarly, Msx2 also helps maintain cell proliferation in optic vesicles and optic cups (Wu et al., 2003). We found that inhibition of COX-2 initially in optic vesicles decreases MSX1 and then gradually increases when the optic cup differentiates into the retina. MSX2 expression rose at the optic vesicle stage and then declined at the optic cup stage. Contrasting regulation of MSX1 and MSX2 during placode to optic vesicle formation indicates that COX-2 interacts with cell proliferation during eye development.

The various transcription factors such as SIX3, VSX2, OTX2 and MITF cause differentiation of neural retina, pigmented retina and lens. SIX3 is expressed in the surface ectoderm before Pax6, and without SIX3, Pax6 is downregulated, and Sox2 is never

expressed (Liu et al., 2006). Here as we observed, PAX6 and SOX2 have altered expression under inhibition of COX-2 and due to this, the expression of SIX3 was also modified. Pax6 triggers the pigmented retina induction and Otx1/Otx2 combined activity when Pax6 and WNT signalling induce the expression of microphthalmia-associated transcription factor (MITF). MITF plays a vital role in the development of melanin-containing cells, melanocytes, and pigmented retina together with Otx proteins (Martínez-Morales et al., 2003). During optic vesicle formation, the expression of OTX2 was less, and at the next stage, it increased, followed by the differentiation stage, where again a decline was observed in etoricoxib-treated embryos, which was observed in the morphology of the developing eye. Vsx2 was needed for early optic cup growth, and removal of Vsx2 resulted in ventral optic cup/stalk deformities. We also found deformities related to the optic cup when COX-2 activity was hampered. VSX2 levels decreased consecutively in all three stages when the embryos were exposed to etoricoxib. MITF also showed low expression throughout the eye development in COX-2-inhibited embryos.

The overall alterations in WNT/ β -catenin signaling and downstream molecules of the BMP and FGF caused defective optic cup patterning if COX-2 is absent. The results indicate that the interaction of COX-2 with WNT, BMP and FGF majorly influences signaling during optic cup morphogenesis.

‘From so simple a beginning endless forms most beautiful & most wonderful have been and are being evolved.’

-Charles Darwin (Origin of Species)

Tables:

Table 5.1: COX-2 activity of control and treated embryos during HH12, HH14 and HH16 stages of development.

Days of isolation	Activity (nmol/min/ml)	
	Control	Treatment
HH12	0.953±0.0004	0.682±0.0121***
HH14	0.459±0.0059	0.358±0.0134**
HH16	0.958±0.0029	0.149±0.0094***

Enzyme activity are expressed as Mean±SEM, n=3 with 30 eggs per group per day; **p≤0.01; ***p≤0.001

Table 5.2: Transcript levels on HH12 stage of development in control and etoricoxib treated embryos.

Gene	Fold change
<i>WNT11</i>	1.0476±0.0196
<i>FZD5</i>	2.9218±0.2430*
<i>FGF8</i>	0.6216±0.0655
<i>FGF9</i>	2.0019±0.8227
<i>BMP7</i>	1.5219±0.2444
<i>BMP4</i>	1.6214±0.0335**
<i>SHH</i>	0.5117±0.0350**
<i>SOX2</i>	1.0040±0.1192
<i>PAX6</i>	0.6398±0.1557
<i>MSX1</i>	0.7287±0.1562
<i>MSX2</i>	1.0072±0.0515
<i>DELTA</i>	1.3770±0.0454*
<i>SIX3</i>	1.6325±0.9658
<i>VSX2</i>	0.7265±0.0118***
<i>OTX2</i>	0.3548±0.0265**
<i>MITF</i>	0.7695±0.0169***

Fold changes are expressed as Mean±SEM. Fold change values for the control embryo is 1.0 for all the genes, n=3 with 30 eggs per group per day; *p≤0.05; **p≤0.01; ***p≤0.001

Table 5.3: Transcript levels on HH14 stage of development in control and etoricoxib treated embryos

Gene	Fold change
<i>WNT11</i>	3.0711±0.2375*
<i>FZD5</i>	1.3091±0.2134
<i>FGF8</i>	0.6586±0.0158**
<i>FGF9</i>	1.1486±0.1335
<i>BMP7</i>	0.7169±0.0256*
<i>BMP4</i>	2.6551±0.3685**
<i>SHH</i>	5.7468±1.2524
<i>SOX2</i>	2.4664±0.6407
<i>PAX6</i>	0.4190±0.0679*
<i>MSX1</i>	0.7764±0.3553
<i>MSX2</i>	0.5683±0.0552*
<i>DELTA</i>	0.4280±0.0583*
<i>SIX3</i>	0.4596±0.0369*
<i>VSX2</i>	0.6234±0.0125***
<i>OTX2</i>	0.2365±0.0084**
<i>MITF</i>	0.8621±0.0096***

Fold changes are expressed as Mean±SEM. Fold change values for the control embryo is 1.0 for all the genes, n=3 with 30 eggs per group per day; *p≤0.05; **p≤0.01; ***p≤0.001

Table 5.4: Transcript levels on HH16 stage of development in control and etoricoxib treated embryos.

Gene	Fold change
<i>WNT11</i>	0.5236±0.2682*
<i>FZD5</i>	0.5539±0.0772*
<i>FGF8</i>	1.1566±0.0984*
<i>FGF9</i>	0.5694±0.0701*
<i>BMP7</i>	1.0229±0.0655
<i>FOXD3</i>	0.6647±0.1050
<i>SHH</i>	0.6997±0.1148
<i>SOX2</i>	1.2329±0.0473*
<i>PAX6</i>	2.1732±0.4703
<i>MSX1</i>	1.9718±0.9020
<i>MSX2</i>	1.5803±0.3278
<i>DELTA</i>	1.1052±0.0596*
<i>SIX3</i>	0.4625±0.0152*
<i>VSX2</i>	1.0365±0.9654
<i>OTX2</i>	0.3658±0.0127***
<i>MITF</i>	0.6815±0.1247***

Fold changes are expressed as Mean±SEM. Fold change values for the control embryo is 1.0 for all the genes, n=3 with 30 eggs per group per day; *p≤0.05; ***p≤0.001

Table 5.5. Spot densitometry analysis of the western blot bands on HH12, HH14 and HH16 stage of development in control and treated embryos.

Protein	Band intensity in arbitrary units	
	Control	Treatment
HH12		
β -catenin	63.002±1.476	36.053±0.542***
Shh	65.314±0.400	57.192±0.799***
Pax6	58.766±0.870	38.236±0.655***
Fgf8	69.122±1.584	89.872±1.244***
Fgf10	59.363±0.491	48.058±1.617**
R-cadherin	53.756±1.507	44.601±0.981**
HH14		
β -catenin	64.155±2.726	57.594±4.442
Shh	84.627±0.338	72.831±1.321***
Pax6	57.946±0.836	34.371±0.424***
Fgf8	91.760±1.344	74.691±2.293**
Fgf10	52.320±0.348	48.019±0.768**
R-cadherin	69.875±2.118	32.829±0.298***
HH16		
β -catenin	68.202±2.631	63.754±2.471
Shh	74.359±0.512	73.337±1.928
Pax6	57.941±0.418	47.072±0.585***
Fgf8	78.348±0.624	86.380±1.110**
Fgf10	49.752±1.545	28.356±0.496***
R-cadherin	69.465±3.597	47.191±0.334**

The values are expressed as Mean±SEM; n=3 with 30 eggs per group per experiment; **p≤0.01, ***p≤0.001